# Influence of Solar Activity Cycles on Earth's Climate

Task 6 – Hypothetical Physical Mechanisms

WP501a – Role of TSI

F. Christiansen
Danish National Space Center

September 12, 2005

# Contents

**INTRODUCTION** ..... 3

**TSI AND TROPOSPHERIC TEMPERATURE** ..... 4

**SEA SURFACE TEMPERATURES** ..... 5

**TSI AND GENERAL CIRCULATION MODELS** ..... 8

**CONCLUSIONS** ..... 15

**REFERENCES** ..... 16

## Introduction

The total solar irradiance (TSI) is in a sense the most obvious solar parameter to single out for study when considering the Sun-climate connection. The power input received by the Earth from the Sun is the driver of Earth's climate system and the variations in TSI do correlate well with the variations seen in the climate. However, the brute variations in power received at Earth are not strong enough to explain the variations in climate that are observed. Variations in TSI over a solar cycle of 1.3 $W/m^2$ at the top of the atmosphere translates to 0.23 $W/m^2$ at the surface. With a climate sensitivity of 0.5-0.8 $K/(W/m^2)$ this corresponds to a change in tropospheric temperature of 0.14-0.18 K. The observed variations in tropospheric temperatures over a solar cycle are, however, approximately 0.5 K. For TSI to be the driver of the climate variations observed some sort of amplification or feedback mechanism must therefore be in place.

The influence of TSI on the climate is multifaceted. Variations in TSI translate to different heating in various layers of the atmosphere, heat absorption in the oceans with different time scales from those of the atmosphere, differential heating over land and oceans, etc. These primary influences from TSI will in turn alter such things as atmospheric circulation, water vapor content in the atmosphere, and cloud cover. Effects from these secondary phenomena may then feed back into the energy absorbed by the climate system from solar irradiation, for example via changes in the Albedo, possibly enhancing the effects of TSI variations.

Due to the geographically heterogeneous nature of solar influence on climate and the rather complicated feedback mechanisms involved in solar forcing of the climate any simple explanation of TSI-climate connections is likely to fail, except in limited cases such as variations in sea surface temperature that seem to be at least partly explainable by simple energy balance considerations. Model studies seem therefore to be the best way to proceed.

## TSI and tropospheric temperature

The electromagnetic radiation from the Sun resembles black body radiation at 5770 K. It covers all wavelengths from far infrared to extreme ultra violet; however, the range from 300 nm to 10.000 nm contains more than 99% of the solar output. Total solar irradiance (TSI) is the solar energy flux integrated over the entire spectrum received at the top of the atmosphere at 1 AU. Satellite measurements of TSI started in November 1978 and have been continued since by various instruments. These instruments do not agree to better than 0.2% in the absolute value of TSI (see Figure 1), but in relative changes of TSI they agree to better than 0.01%. Fröhlich and Lean, 1998, and Lee III et al., 1995, have constructed continuous time series of TSI from these satellite data from 1978 to the present.

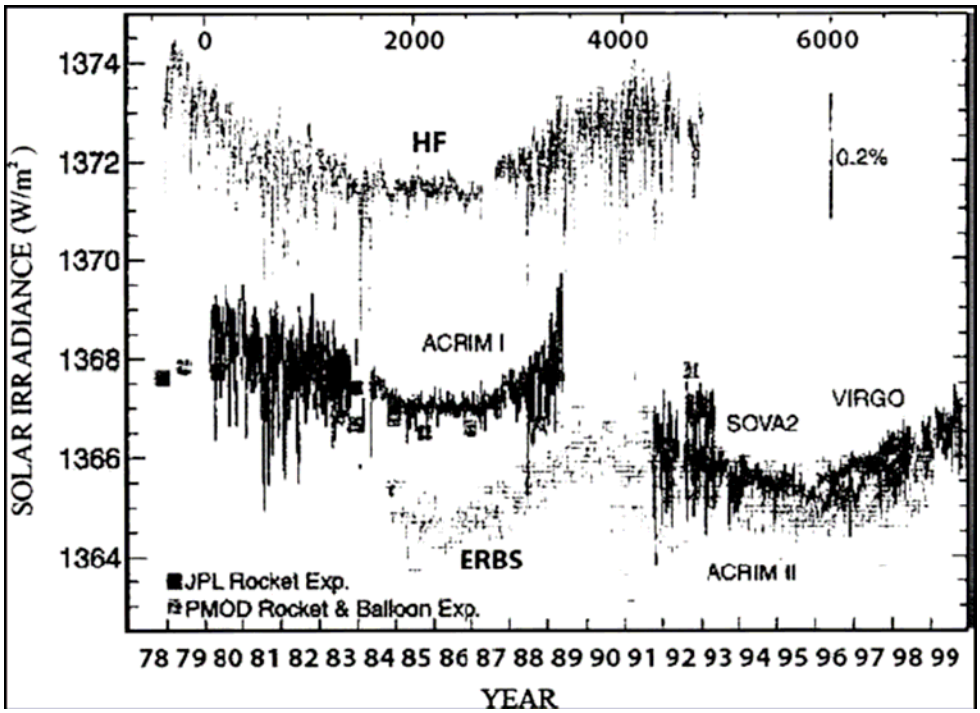


**Figure 1: Daily average values of TSI from a number of radiometer experiments since 1978. From Fröhlich, 2000.**

The "solar constant" value of TSI is at present fluctuating around 1367 W/m$^2$, however variations in TSI exist on many time scales from minutes to millennia. Reconstructions of TSI based on proxy data, e.g., sunspot number, have been constructed going back through the Maunder minimum (Lean et al., 1995, Hoyt and Schatten, 1993, and others). These reconstructions agree qualitatively, though in absolute numbers there are significant differences.

Figure 2 shows TSI together with global mean tropospheric temperature anomaly. The correlation is reasonably good, 0.31, increasing to 0.61 when using a 12 month running mean of both TSI and temperature. Over a solar cycle TSI varies approximately 1.3 W/m$^2$

from solar min to solar max. With the geometric factor of ¼ and the Earth's Albedo of 0.7 this translates to a forcing of the atmosphere of 0.23 $W/m^2$. With a climate sensitivity of 0.6-0.8 $K/(W/m^2)$, (e.g., Appendix 9.1, Houghton et al., 2001), estimated from the average response of climate models to a doubling of CO2 this translates to a response of 0.14-0.18 K between solar max and solar min. However, the tropospheric temperature varies with approximately 0.5 K over a solar cycle. A direct forcing from TSI is therefore not sufficient to explain the variation of tropospheric temperatures and some amplification mechanisms would be required for TSI to be the main driver of the tropospheric temperature variability.

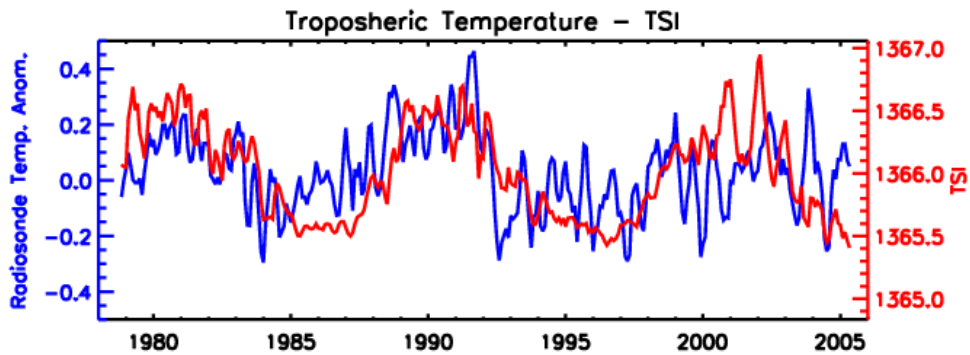


**Figure 2: TSI and global tropospheric temperature anomaly. The temperature data have a linear trend and internal modes of variability removed. Correlation coefficient is equal to 0.31, increasing to 0.61 when using a 12 month running mean.**

## Sea surface temperatures

Sea surface temperatures display some correlation with changing solar activity. Using temperature data from ocean going ships and sunspot number as a measure for solar activity Reid (1987, 1991, 2000) has demonstrated this going back to the mid 19th century. Figure 3 shows the global sea surface temperature anomaly compared to sunspot number. In Figure 4 we show the SST temperature and TSI used in Task 4. The correlation is rather poor, 0.09, increasing only to 0.1 when using 12 month running averages. Introducing a lag increases the correlation to 0.13 for a lag of 12 months.

White et al. (1997) investigated the response of SST to changing solar activity using band-passed-filtered surface marine weather observations (1900-1991) and bathythermograph upper ocean temperature profiles (1955-1994). They found clear signals in power spectra, singular spectrum analysis, and empirical orthogonal functions corresponding to the solar 11- and 22-year cycles, see Figures 5 and 6. Moreover, they found that these signals were consistent across the three major oceanic basins. The band-passed-filtered data for the SST anomalies yielded solar-related components with amplitudes of 0.04 K and 0.07 K for the 11-year and 22-year cycles, respectively, associated with TSI amplitudes of 0.5 $W/m^2$ at the top of the atmosphere (1.0 $W/m^2$ max to min difference) corresponding to a climate sensitivity of the oceans of 0.08-0.14 $K/(W/m^2)$.

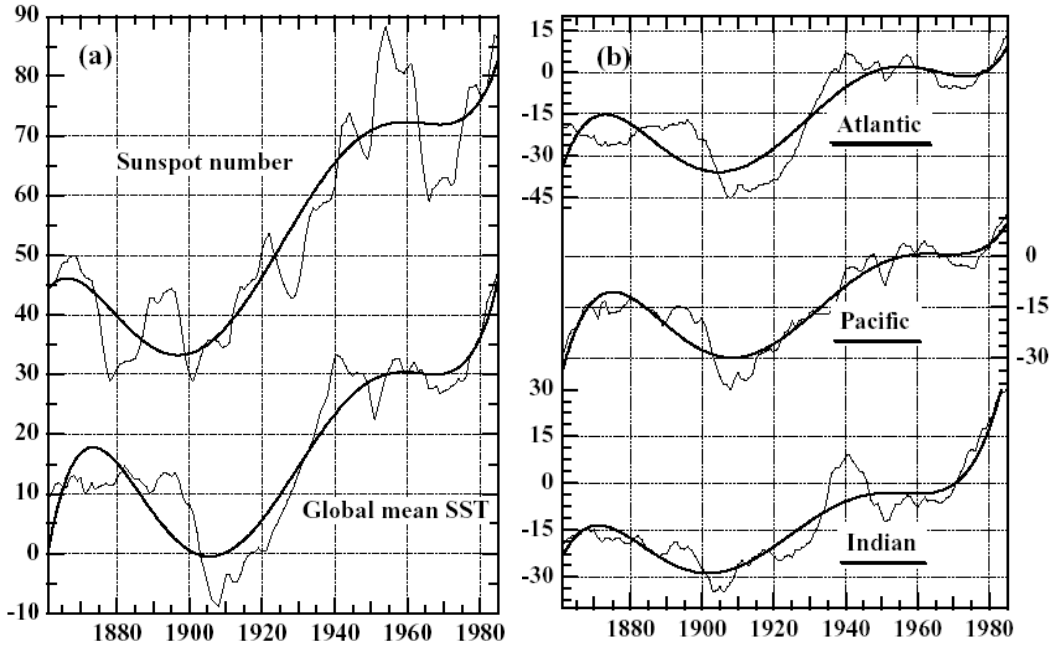


**Figure 3: From Reid (2000). Sea surface temperature anomalies in 0.01 K (lower left: global average, right: basin averages) compared to sunspot number (upper left). To emphasize to the long term similarity between the data sets 7th degree polynomia (fat) have been fitted to the curves.**

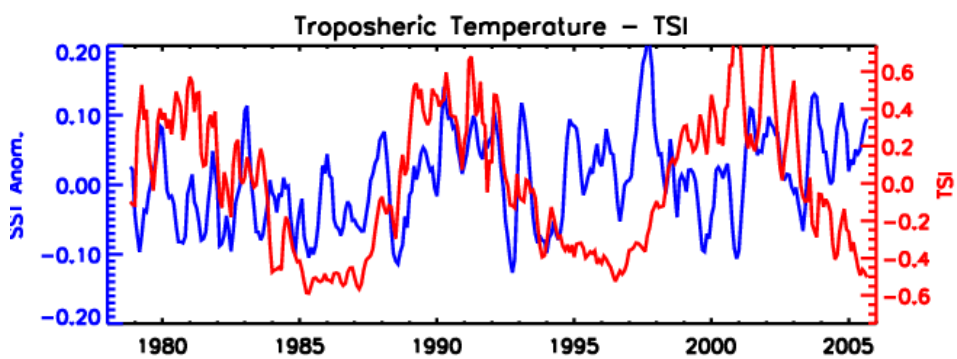


**Figure 4: SST and TSI. The correlation over the past 25 years is rather poor with a coefficient of 0.09.**

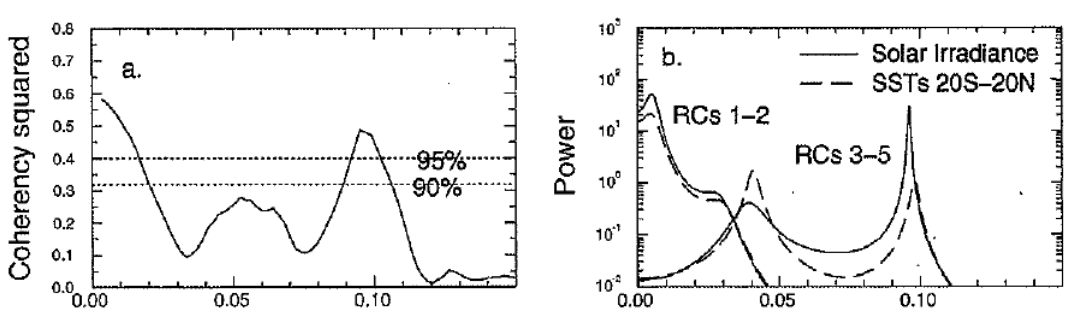


**Figure 5: From White et al. (1997). Left: coherency spectrum for annual time series of global SST and TSI anomalies. Right: Maximum entropy spectrum of leading reconstructed components from two-channel singular spectrum analysis of SST and TSI. The peaks correspond to approximately 11- and 22-year cycles.**

White et al. (1997) then consider the global average heat budget of the upper ocean (Gill, 1982) $\partial T/\partial t + KT = S/(\rho CH)$, where T is the temperature anomaly, S is the irradiance anomaly at the sea surface, ρ and C are the density and specific heat of sea water, H is the depth the solar signal penetrates uniformly into the upper ocean, and K is the inverse of the dissipation time scale. $K^{-1}$ is estimated from the time lags observed in the singular spectrum analysis to be 1-1.5 years for the 11-year cycle and 2-3 years for the 22-year cycle and the penetration depth H is correlations in the bathythermograph data to be 40-60 m for the 11-year cycle and 40-80 m for the 22-year cycle. This results in an upper ocean response to a top of the atmosphere TSI signal of 0.5 $W/m^2$ of 0.01-0.03 K for the 11-year cycle and 0.02-0.05 K for the 22-year cycle. Furthermore, they find that the phase lags observed agree well with what comes out of considering the equilibration time scale from a Stefan-Boltzmann law calculation.

The model derived estimates of the sensitivity of the ocean temperatures to a TSI signal of 0.5 $W/m^2$ of is on the low side, 0.01-0.03 K compared to the observed 0.04 K for the 11-year cycle, and 0.02-0.05 K compared to the observed 0.07 K for the 22-year cycle. The simplicity of the model, however, may well be responsible for this. Feedback mechanisms with the atmosphere could change the model response to agree better with the observations.

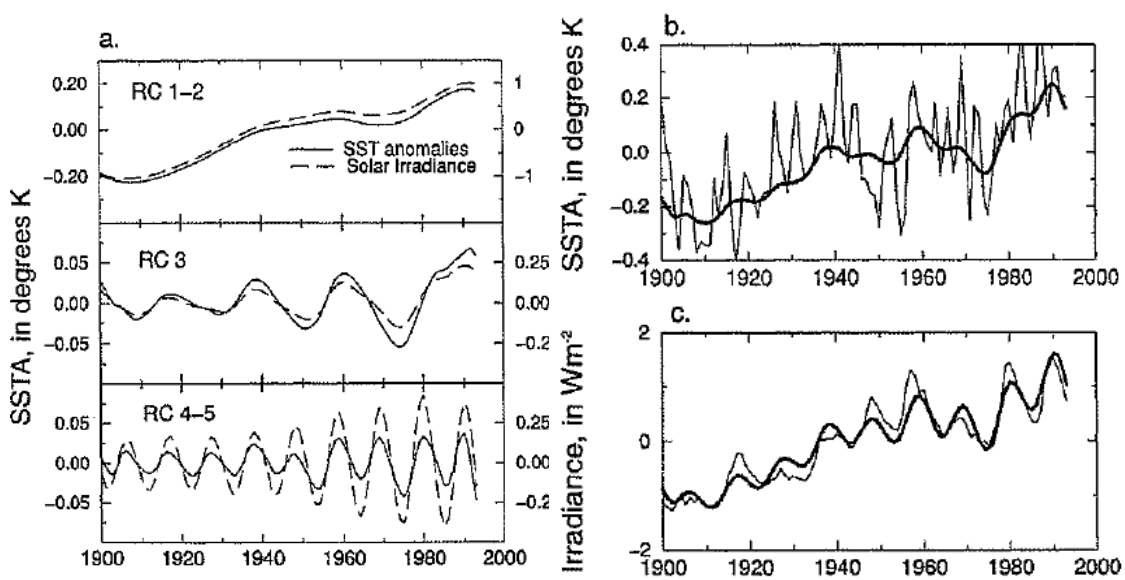


**Figure 6: From White et al. (1997). Reconstructed components from singular spectrum analysis of SST and TSI. Left: the RCs of SST and TSI for RC=1-2, RC=3 and RC=4-5. Right: The RCs 1-6 for SST and TSI (fat curve) compared to the unfiltered data. The SST still have a considerable signal not account for by the RCs 1-6 whereas TSI is well described by RC 1-6.**

## TSI and General Circulation Models

There are a large number of studies with the effects of changing TSI in general circulation models. Haigh (1999) gives a short introduction to some of these results. In general, the models all reproduce an increase in global average surface air temperature with increasing solar radiation, however they differ strongly in the geographical distribution of this warming, e.g., showing stronger responses in South America and the Arctic Ocean (Rind and Overpeck, 1993), mid- to high-latitudes (Nesme-Rimes et al., 1993), or northern hemisphere land areas (Cubasch et al., 1997). Haigh comments that the lack of a clear pattern between the models is an indicator "that the physical representations, in at least some of the models, are inadequate to the task."

Stott et al. (2003) suggest that models may underestimate the solar contribution to recent climate change. They suggest that the methodology of earlier optimal detection analyses comparing model-simulated climate change with observations could have a bias against weak climate signals lost in the sampling noise. If that is the case these earlier studies could have underestimated the importance of natural factors and attributed a larger effect to anthropogenic causes of climate change. In order to avoid this they made model runs of a GCM with artificially increased changes in TSI and volcanic stratospheric aerosols (VOL) (10-fold for TSI and 5-fold for VOL). The results are shown in Figure 7. It is interesting to note the relatively large discrepancy between the LBB curve (TSI reconstructed by Lean et al., 1995) and the HS curve (TSI reconstructed by Hoyt and Schatten, 1993) from 1900 to 1960.

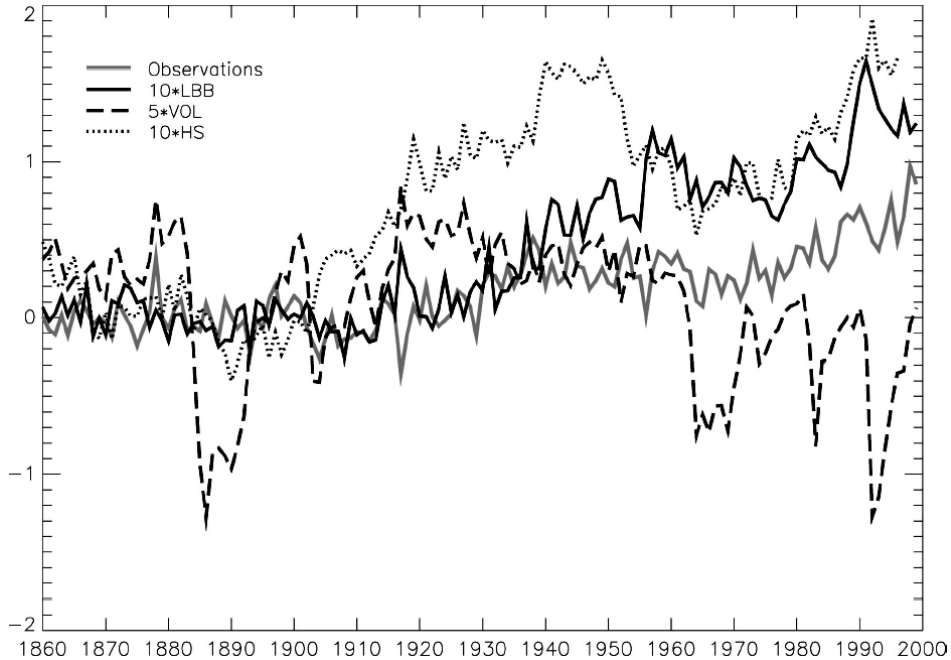


**Figure 7: Global mean near surface temperature anomalies as a result from forcing with 10-fold enhanced TSI variations from Lean et al. (1995) (LBB) and from Hoyt and Schatten (1993) (HS), 5-fold enhanced stratospheric aerosols from Sato et al. (1993) (VOL) and observations.**

The model runs with the artificially enhanced natural forcings are then regressed together with ordinary runs with forcings from greenhouse gas and sulfur emissions with the observed global mean temperature anomalies giving rise to a set of linear regressions coefficients that attribute relative importance to each of the forcing mechanisms. Compared to a similar set of regression coefficients from ordinary model runs with (non-enhanced) natural forcings the results differ significantly. Using the enhanced LBB data for TSI suggests an increase in relative importance of TSI by a factor 2.64, whereas the same factor is 1.96 for the HS reconstruction of TSI. At the same time the relative importance of GHG is decreased by a factor of 0.81 (LBB) and 0.60 (HS). This result could potentially go some way to explain the discrepancy between the climate model sensitivity to changes of TSI and the observed temperature fluctuations. The authors have some caveats and reservations about their results but note that the conclusion is supported by two other studies. Hill et al. (2001) find that models underestimate the solar response in tropospheric temperatures by a factor of 2 to 3, and North and Wu (2001) find an underestimate for near-surface temperatures of about 2.

Meehl et al. (2003) have investigated the climate response over the 20$^{th}$ century to both solar and greenhouse gas forcing. Using model runs of a fully coupled global ocean-atmosphere-sea ice-land surface model (Washington et al. 2000), with forcings from greenhouse gases+sulfate, from solar variations (TSI from Hoyt and Schatten, 1993), and from both they produced the global temperature anomalies shown in Figure 8. The combination of GHG+sulfate and solar forcing reproduces the observed surface temperature anomalies fairly well.

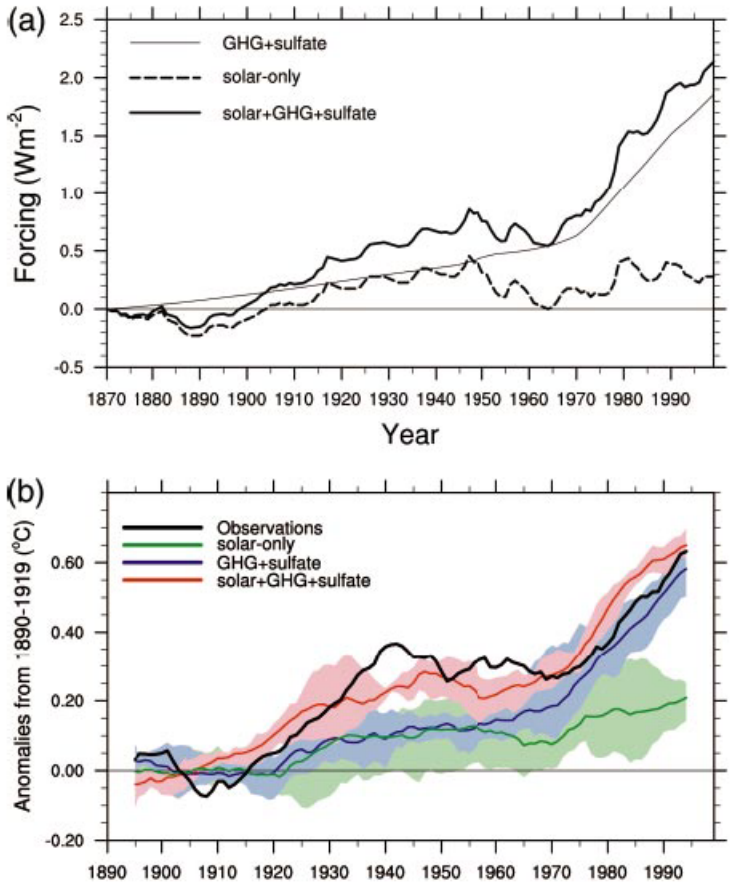


**Figure 8: From Meehl et al., 2003. (a) Top of the troposphere radiative forcing used in the model for GHG+sulfate, solar, and both. (b) Global annual mean surface air temperature for observations and model outputs. Only the combined GHG and solar forcing reproduces the observations.**

The authors use the separate runs for solar, GHG+sulfate, and solar+GHG+sulfate to focus on the seasonal and regional response for solar forcing in the early 20$^{th}$ century and GHG+sulfate late in the century. Of particular importance is an apparent non-linear effect of the solar forcing that is seen when comparing model runs with solar forcing only and residuals between model runs with solar+GHG+sulfate and GHG+sulfate only. The study shows that the effects of the solar forcing are considerably larger in the latter case, i.e., when the solar forcing is working together with greenhouse gases. In Figure 9 the effects of solar+GHG+sulfate and GHG+sulfate and their difference (solar residual) is shown. The increased warming arising from the solar forcing occurs mainly at northern hemisphere high altitudes, with a maximum of 0.7 K in the late 1940s. This is an effect associated with an ice-Albedo feedback that has been observed in other model studies. To demonstrate the non-linear effect of using solar forcing only (Figure 10) and solar forcing combined with GHG+sulfate (Figure 11) the authors focus on the early 20$^{th}$ century where the solar forcing increases strongly. The figures show net changes over the period in solar irradiance absorbed at the surface, IR at the surface, and total cloud cover.

Top of Figure 10 shows that though the solar irradiation has increased over the early 20$^{th}$ century this has not resulted in a net increase in solar irradiation absorbed at the surface. Small increases over the oceans are offset by similar decreases over land. This is associated with increases in cloud cover over land. The net infrared radiation has

consistently increased with a similar effect whether the forcing is solar or GHG+sulfate. This increase in infrared radiation can be explained by ocean warming resulting in increases in water vapor and cloud cover over both land and oceans.

The response is quite different when the solar forcing is calculated as the difference between solar+GHG+sulfate and GHG+sulfate only. Now, the net solar radiation absorbed at the surface is consistently increasing over the early 20$^{th}$ century. At least for northern summer this is consistent with a decrease in cloud cover. It is also interesting to note that the land-ocean differential in net solar radiation is stronger in the solar residual case and that this could enhance the land-sea temperature gradients. Combined with the corresponding changes in net IR at the surface the solar-residual has a larger land forcing contrast in the northern summer season than the solar only case, and this possible non-linear behavior could have an effect on tropical monsoon areas.

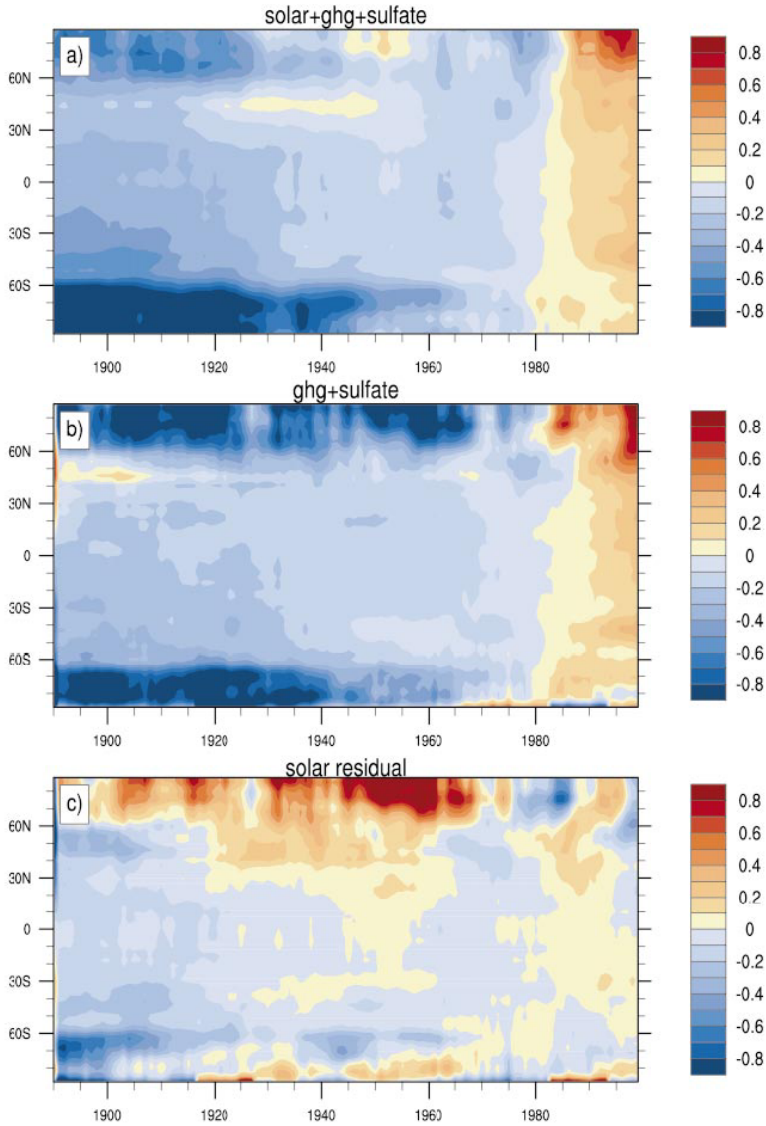


**Figure 9: From Meehl et al. (2003). 10-yr running mean zonal surface temperature anomalies. Top: forcing with solar+GHG+sulfate. Middle: GHG+sulfate forcing only. Bottom: solar residual, i.e., top-middle.**

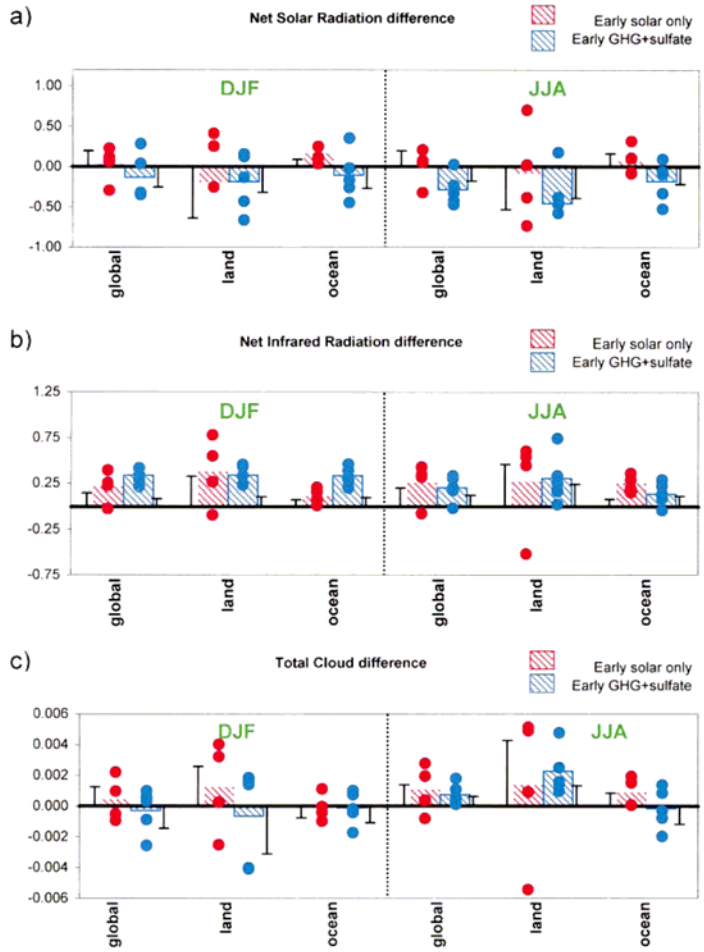


**Figure 10: From Meehl et al. (2003). Net solar (top) and infrared (middle) radiation and cloud cover (bottom) differences from model ensemples for early 20th century with solar only (red) and GHG+sulfate (blue). Left: Northern winter. Right: Northern summer. The boxes are ensemble means, the dots are individual ensemble members.**

Figure 12 shows the precipitation differences over the West African and South Asian monsoon regions for solar only and solar residual forcing during the early 20$^{th}$ century. The solar residual case displays significant increases in precipitation compared to the solar only case. The authors note that the increase in precipitation over the South Asia monsoon region is consistent with the all-India monsoon index.

Solar forcing is spatially heterogeneous and can create feedbacks in the regional circulation regimes. Over the relatively cloud-free subtropical oceans regions enhanced solar radiation will produce greater evaporation leading to increased rainfall in the precipitation regions creating a feedback via intensified upward vertical motion of the regional Hadley and Walker cells. This in turn leads to fewer clouds over the subtropical ocean regions and an even stronger increase in solar radiation received at the surface.

The authors trace the non-linear effect from combining solar and anthropogenic forcing to an increase in sea surface temperatures of 0.2-0.3 K produced by GHG+sulfate forcing

in the subtropical oceans. This increase in SST intensifies the regional feedback mechanism from solar forcing.

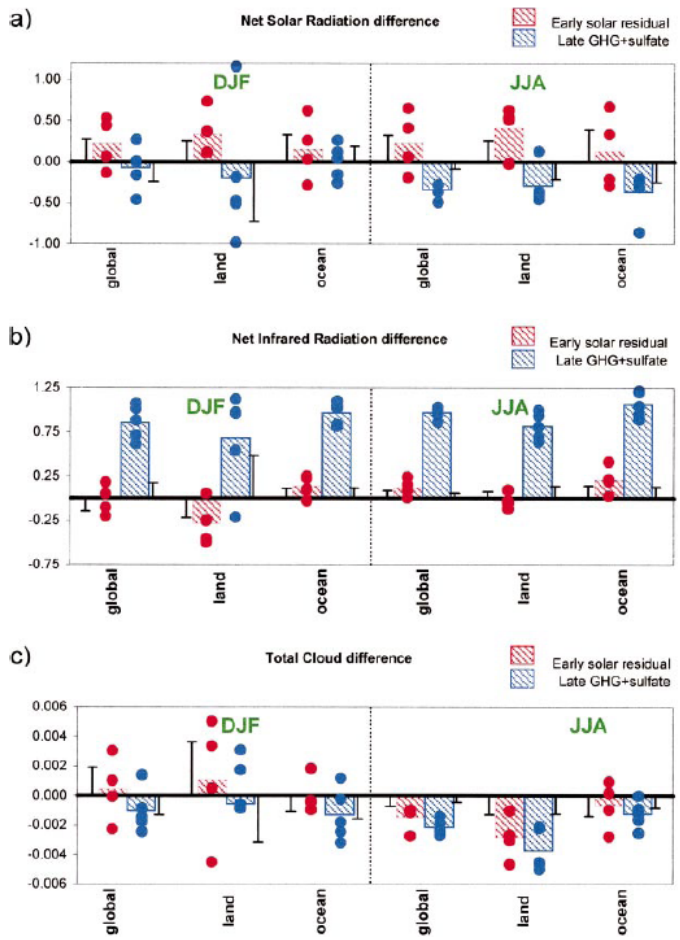


**Figure 11: From Meehl et al. (2003). Same as Figure 10 but for solar residual (red) and late 20th century GHG+sulfate forcing.**

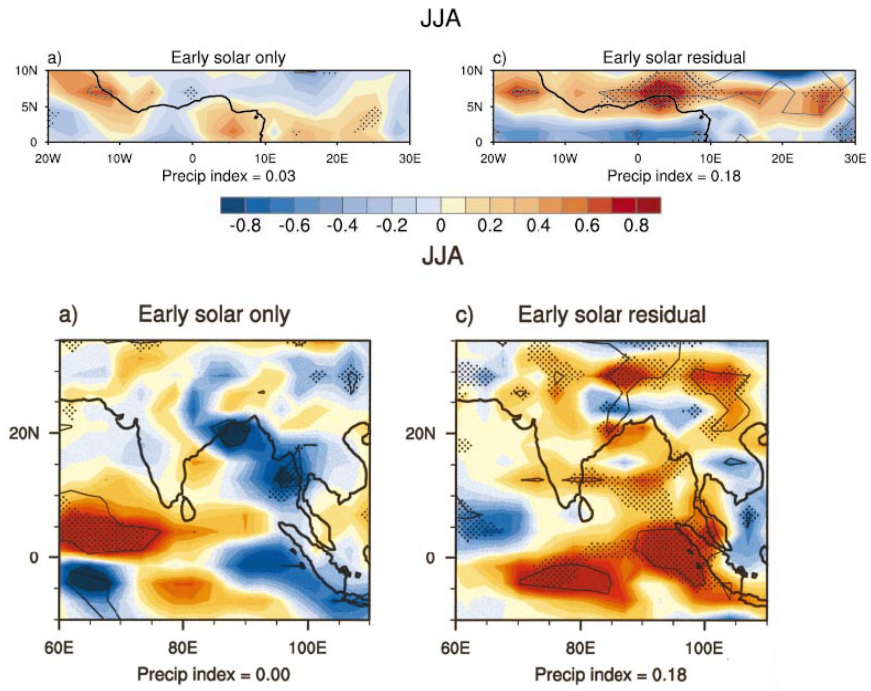


**Figure 12: From Meehl et al. (2003). Precipitation differences (mm/day) in the West African (top) and South Asian (bottom) monsoon regions over the early 20th century for solar only (left) and solar residual (right).**

## Conclusions

Model considerations show that the climate sensitivity to changes in total solar irradiation is too small by factor of 3 to explain the variations observed in surface and tropospheric temperatures.

Contrary to this, it seems to be possible to explain the (solar cycle) variations in sea surface temperatures with changes in solar irradiation. When band-pass-filtering sea surface temperatures to single out the variations that follow the solar 11-year and 22-year cycles it is possible to explain these variations from simple energy balance considerations (White et al., 1997). The derived sensitivity of SST to changes in TSI is somewhat on the low side compared to the variations actually observed, but the simplicity of the energy balance model could be the explanation of this.

Model studies of the influence of TSI on atmospheric temperatures do not show a consistent picture. However, Stott et al. (2003) suggest that climate models may underestimate the role of solar forcing in climate change because the effects are lost in the ensemble sample noise when using optimal detection of the relative importance of various forcings – greenhouse gases, aerosols, solar, etc. They therefore tried model runs with artificially increased variations in solar radiation. When combining these enhanced solar signals with other factors such as anthropogenic forcing they saw an increase in the importance related to climate variations of the solar signals by a factor of 2-3, when compared to using non-enhanced signals.

Meehl et al. (2003) make some very interesting points about non-linear effects of combining solar forcing with anthropogenic forcing. Anthropogenic forcing raises the base level sea surface temperatures in the subtropical oceans. The increased evaporation strengthens the feedback mechanisms involved in the influence of solar forcing of particularly the monsoon regions, changing the regional cloud cover, rainfall and circulation.

## References


Frohlich, C. and J. Lean, The Sun's total irradiance: Cycles, trends and related climate change uncertainties since 1976, *Geophysical Research Letters, 25*(23), 4377-4380, 1998.

Cubasch, U., R. Voss, G.C. Hegerl, J. Waszkewitz, and T.J. Crowley, Simulation of the influence of solar radiation variations on the global climate with an ocean-atmosphere general circulation model, *Clim. Dyn., 13*, 757-767,1997.

Fröhlich, C., Observations of irradiance variations, *Space Science Review 94*,15–24, 2000.

Gill, A.E., *Atmosphere-Ocean Dynamics*, Academic, San Diego, California, 1982.

Haigh J.D., Modelling the impact of solar variability on climate*, J. Atmos. Sol.-Terr. Phys., 61*(1-2), Pages 63-72, 1999.

Hill, D. C., M. R. Allen, N. P. Gillett, S. F. B. Tett, P. A. Stott, G. S. Jones, W. J. Ingram, and J. F. B. Mitchell, Natural and anthropogenic causes of recent climate change. Detecting and Modelling Regional Climate Change, M. B. India and D. L. Bonillo, Eds., Springer-Verlag, 275–290, 2001.

Houghton J.T., Y. Ding, D.J. Griggs, M. Noguer, P.J. van der Linden, D. Xiaosu, Climate Change 2001: The Scientific Basis. Cambridge University Press, 2001.

Hoyt, D. V. and Schatten, K. H., A discussion of plausible solar irradiance variations, 1700-1992. *Journal of Geophysical Research 98*, 18 895-18 906, 1993.

Lean, J., Beer, J. & Bradley, R. S., Reconstruction of solar irradiance since 1610: implications for climate change. *Geophysical Research Letters 22*, 3195-3198, 1995

Lee III, R. B., M. A. Gibson, R. S. Wilson, and S. Thomas, Long-term total solar irradiance variability during sunspot cycle 22, *Journal of Geophysical Research, 100*(A2), 1667–1675, 1995.

Meehl, G.A., W.M. Washington, T.M.L. Wigley, J.M. Arblaster, A. Dai, Solar and Greenhouse Gas Forcing and Climate Response in the Twentieth Century*, J. of Clim., 16*, 426-444, 2003.

Nesme-Rimes, E., E.N. Ferriera, R. Sadourny, H. LeTreut, and Z.X. Li, Solar dynamics and its impact on solar irradiance and the terrestrial climate*, J. Geophys. Res., 98,* 18923-18935, 1993.

North, G. R., and Q. Wu, Detecting climate signals using space–time EOFs., *J. Climate*, *14*, 1839–1863, 2001.

Reid G.C., Influence of solar variability on global sea surface temperatures, *Nature, 329,* 142-143, 1987.

Reid, G.C., Solar total irradiance variations and the global sea surface temperature record, *Journal of Geophysical Research, 96*, 2835-2844, 1991

Reid G.C., Solar variability and the Earth's climate: Introduction and overview, *Space Science Review, 94*, 1-11, 2000.

Rind, D. and J. Overpeck, Hypothesised causes of decade-to-century-scale climate variability: climate model results, *Quat. Sci. Rev*., 12, 357-374, 1993.

Sato, M., J. E. Hansen, M. P. McCormick, and J. B. Pollack, Stratospheric aerosol optical depths (1850–1990). *J. Geophys. Res*., 98**,** 22 987–22 994, 1993.

Stott P.A., G.S. Jones, and F.B. Mitchell, Do models underestimate the Solar contribution to recent climate change?, *Journal of Climate., 16*, 4079-4093, 2003.

Washington, W.M., et al., Parallel climate model (PCM) control and transient simulations, *Climate Dynamics, 16,* 755-774.

White, B.W., J. Lean, D.R. Cayan, and M.D. Dettinger, Response of global upper ocean temperature to changing solar irradiance, *Journal of Geophysical Research, 102*(C2), 3255-3266.